INTERNATIONAL JOURNAL FOR NUMERICAL METHODS IN FLUIDS
*Int. J. Numer. Meth. Fluids* 2019; **00**:1–16
Published online in Wiley Online Library (www.onlinelibrary.wiley.com). DOI: 10.1002/fld.4740

# Capturing the Cross-Terms in Multi-Dimensional Advection Schemes

James Kent*

*Computing and Mathematics, University of South Wales, Pontypridd, United Kingdom*

SUMMARY

Solving the advection equation is an important part of numerically modelling the atmosphere. Both accuracy and efficiency are desirable traits of an advection scheme. For multi-dimensional flow, forward-in-time advection schemes must properly capture the cross-terms. Failure to capture the cross-terms can result in reduced accuracy and even instabilities. We show how multi-dimensional forward-in-time schemes successfully capture the cross-terms of two-dimensional flow. We then introduce a method to improve the efficiency of the forward-in-time schemes for two-dimensional flow. This method stacks the duplicated cross-terms from one flux into the other, creating asymmetrized fluxes. Numerical testing shows that these asymmetrized flux calculation schemes perform to the same accuracy as the original forwards-in-time schemes but with a significant improvement in computational time. Finally, we show extensions of the method to three-dimensional flow. 

Received . . .

KEY WORDS: Transport, Finite-Difference, Finite-Volume, Advection, Atmospheric Modelling

## 1. INTRODUCTION

Advection appears in all branches of computational fluid dynamics, and is especially prominent in numerical models of the atmosphere and the oceans. Numerical advection schemes can be used for advective transport, for solving conservation laws, and in the solution of the momentum equations. The focus in this paper is primarily on advective transport. There are a number of different numerical methods (for example, finite-difference [Crowley(1968)], finite-volume [Lin and Rood(1996)], finite-element [Melvin et al.(2012)], semi-Lagrangian [Staniforth and Côté(1991)], and Lagrangian [Bosler et al.(2017)], see [Rood(1987)], [Lauritzen et al.(2011)] and references within) that can be used to solve the advection equation for transport problems.

The advection equation is given by

$$q_t + \mathbf{u} \cdot \nabla q = 0, \tag{1}$$

where $q$ is the advected quantity (called the tracer mixing ratio), $t$ is time, $\mathbf{u}$ is the velocity vector, and the subscript indicates a derivative. The transport of a density $\Phi$ is governed by the conservation

*Correspondence to: James Kent, University of South Wales, Pontypridd, CF37 1DL, United Kingdom. Email: james.kent@southwales.ac.uk

law

$$\Phi_t + \nabla \cdot (\mathbf{u}\Phi) = 0. \tag{2}$$

For the mass continuity equation $\Phi = \rho$, where $\rho$ is the fluid density, and for the conservative advection equation $\Phi = \rho q$ (i.e. the tracer density). For non-divergent velocities, $\nabla \cdot \mathbf{u} = 0$, then the advection equation can be written in flux form using $\Phi = q$.

There are three important properties for any advection scheme used by a numerical model; accuracy, efficiency and stability. The stability of a numerical scheme is vital, whereas accuracy and efficiency are desirable traits that often impact each other. In general, high-order accurate schemes are less efficient than low-order schemes. One method to decrease computational time, while retaining accuracy, is through the use of parallel computing. In this paper we focus on decreasing computational time through improving the efficiency of a numerical scheme. We do not consider parallel performance.

For multi-dimensional flow it is important that an advection scheme captures the effects of the flow in all coordinate directions as well as the *cross* flow. For forward-in-time advection schemes, e.g. those similar to Lax-Wendroff [Lax and Wendroff(1960)] and ADER schemes [Toro et al.(2001)], the terms depending on multiple directions are denoted the *cross-terms*. Failure to include the cross-terms, such as using strictly one-dimensional methods to compute the fluxes, can lead to a decrease in accuracy and even instabilities in the numerical scheme [Leonard et al.(1996)]. There have been a number of methods designed to try and capture the cross-terms at reduced cost, such as time-splitting [Crowley(1968), Tremback et al.(1987)] and the Lin-Rood scheme [Lin and Rood(1996)], as well as methods designed to capture the cross-terms on unstructured grids [0, Lamine and Edwards(2013)]. Also, using other time stepping methods such as Runge-Kutta can capture the cross-terms even if one-dimensional methods are used to compute the fluxes [Katta et al.(2015)]. For forward-in-time schemes, the method of explicitly calculating each term individually can be achieved by taking the one-dimensional Lax-Wendroff scheme and extending into two-dimensions [Smolarkiewicz(1982)]. The drawback to this method is that for higher-order versions of the Lax-Wendroff scheme, see [Tremback et al.(1987)], the extension into two-dimensions can be prohibitively expensive (leading to the trade off between efficiency and accuracy). Forward-in-time advection schemes can generally be written in conservative form (2), and in this case the cross-terms must be captured in the numerical fluxes. In this paper we provide a method for stacking the duplicated terms to create asymmetrized fluxes, and therefore improving the efficiency of these schemes.

In this paper the methods are demonstrated for two-dimensional flow. In two-dimensions the advection equation is given by

$$q_t + uq_x + vq_y = 0, \tag{3}$$

where $u$ and $v$ are the velocities in the $x$ and $y$ direction respectively. The flux form becomes

$$\Phi_t + (u\Phi)_x + (v\Phi)_y = 0. \tag{4}$$

For all cases within this paper we consider a doubly periodic domain of size 1.

Section 2 derives the forward-in-time schemes and shows how the multi-dimensional schemes capture the cross-terms. Improving the efficiency of the forward-in-time schemes by using the asymmetrized flux calculation is described in Section 3. Numerical testing of the asymmetrized flux schemes, compared with the corresponding usual formulation, is in Section 4. Extending the method to three-dimensional flow is in Section 5, and the summary and conclusions are given in Section 6.

## 2. FORWARD-IN-TIME SCHEMES FOR TWO-DIMENSIONAL FLOW

In this section we derive the standard forward-in-time method. Forward-in-time methods make use of the data at time level $n$ to predict data at the new time level $n+1$ [Durran(2010)]. They are designed such that the temporal order-of-accuracy is equal to the spatial order-of-accuracy (and

arbitrarily-high order can be achieved). This is in contrast to other time stepping methods, such as leapfrog or Runge-Kutta, where the temporal order-of-accuracy is fixed. There are a number of different ways to derive the forward-in-time formulation, and here we focus on Taylor series expansions with constant velocities.

Taylor expansions on $q_{ij}^{n+1}$ gives

$$q_{ij}^{n+1} = q_{ij}^{n} + \Delta t q_t + \frac{\Delta t^2}{2!} q_{tt} + \frac{\Delta t^3}{3!} q_{ttt} + \frac{\Delta t^4}{4!} q_{tttt} + ... + \frac{\Delta t^p}{p!} \frac{\partial^p q}{\partial t^p} + ... \tag{5}$$

where $n$ is the temporal index, $i$ and $j$ are the spatial indices, $p$ is an arbitrary order, and $\Delta t$ is the temporal step size. The derivatives are evaluated at the grid point with indices $i, j$.

We can now calculate the temporal derivatives in terms of the advection equation (3). For the case of constant $u$ and $v$

$$q_t = -uq_x - vq_y, \qquad \text{and} \qquad q_{tt} = -uq_{xt} - vq_{yt}. \tag{6}$$

Substituting expressions for spatial derivatives gives

$$q_{tx} = -uq_{xx} - vq_{yx}, \qquad q_{ty} = -uq_{xy} - vq_{yy}, \qquad q_{tt} = u^2 q_{xx} + 2uvq_{xy} + v^2 q_{yy}, \tag{7}$$

which when substituted into (5) gives a second-order approximation of $q_{ij}^{n+1}$ as

$$q_{ij}^{n+1} = q_{ij}^{n} - \Delta t \left(uq_x + vq_y\right) + \frac{\Delta t^2}{2!} \left(u^2 q_{xx} + 2uvq_{xy} + v^2 q_{yy}\right) \tag{8}$$

The mixed derivative in the $\Delta t^2$ terms is classed as a cross-term because it is multi-dimensional and requires both $x$ and $y$ derivatives. The approximation of $q_{ij}^{n+1}$ can be taken to higher order, resulting in multiple cross-terms. The coefficients of temporal derivatives in terms of spatial derivatives can be taken from Pascal's triangle, and to fourth-order this becomes

$$\begin{aligned} q_{ij}^{n+1} = q_{ij}^{n} &- \Delta t \left(uq_x + vq_y\right) + \frac{\Delta t^2}{2!} \left(u^2 q_{xx} + 2uvq_{xy} + v^2 q_{yy}\right) \\ &- \frac{\Delta t^3}{3!} \left(u^3 q_{xxx} + 3u^2 vq_{xxy} + 3uv^2 q_{xyy} + v^3 q_{yyy}\right) \\ &+ \frac{\Delta t^4}{4!} \left(u^4 q_{xxxx} + 4u^3 vq_{xxxy} + 6u^2 v^2 q_{xxyy} + 4uv^3 q_{xyyy} + v^4 q_{yyyy}\right) \end{aligned} \tag{9}$$

A numerical advection scheme must capture each of these terms to be formally fourth-order accurate for constant advection. For example, approximating each of these derivatives using fourth-order finite-differences will result in an advection scheme which is fourth-order accurate in both space and time. The above result can also be derived using the ADER method (see, for example, [Toro et al.(2001)] and [Norman and Finkel(2012)]), and the ADER derivation shows that this holds for non-constant velocities $u$ and $v$.

A common approach to solving the advection equation (3) with forward-in-time schemes is to calculate values of the advected quantities inbetween grid points at grid cell edges. Letting $\hat{q}$ denote the value of $q$ at the flux points (half indices in their respective directions), with the superscript indicating which direction, then the solution can be approximated using

$$q_{ij}^{n+1} = q_{ij}^{n} - u_{ij} \frac{\Delta t}{\Delta x} \left(\hat{q}^x_{i+\frac{1}{2}j} - \hat{q}^x_{i-\frac{1}{2}j}\right) - v_{ij} \frac{\Delta t}{\Delta y} \left(\hat{q}^y_{ij+\frac{1}{2}} - \hat{q}^y_{ij-\frac{1}{2}}\right) \tag{10}$$

where $\Delta x$ and $\Delta y$ are the grid spacings in the $x$ and $y$ directions respectively, and $q$ is stored at integer grid indices. The discretization of the terms $\hat{q}^x$ and $\hat{q}^y$ determines the properties (such as order-of-accuracy and monotonicity) of the forward-in-time scheme.

Similarly, the flux form equation (4) can be solved

$$\Phi_{ij}^{n+1} = \Phi_{ij}^{n} - \frac{\Delta t}{\Delta x} \left((u\hat{\Phi}^x)_{i+\frac{1}{2}j} - (u\hat{\Phi}^x)_{i-\frac{1}{2}j}\right) - \frac{\Delta t}{\Delta y} \left((v\hat{\Phi}^y)_{ij+\frac{1}{2}} - (v\hat{\Phi}^y)_{ij-\frac{1}{2}}\right). \tag{11}$$

The fluxes here are $F = u\hat{\Phi}^x$ and $G = v\hat{\Phi}^y$, and so $\hat{\Phi}^x$ and $\hat{\Phi}^y$ are the cell edge values of $\Phi$. As conservation is a desired property of an advection scheme, in practice the flux-form of the equations is commonly used (with $\Phi = \rho q$ being the tracer density). However, for clarity of the derivation we will focus on the advective form here. It is clear that for a fourth-order scheme $\hat{q}^x$ and $\hat{q}^y$ must be discretized such that their use in equation (10) contains approximations to the terms given in (9). The question is how to discretize $\hat{q}^x$ and $\hat{q}^y$ to capture these terms? As $\left(\hat{q}^x_{i+\frac{1}{2}j} - \hat{q}^x_{i-\frac{1}{2}j}\right)/\Delta x$ and $\left(\hat{q}^y_{ij+\frac{1}{2}} - \hat{q}^y_{ij-\frac{1}{2}}\right)/\Delta y$ are discrete approximations to $\hat{q}^x_x$ and $\hat{q}^y_y$ around the point with index $ij$, one option would be to choose $\hat{q}^x$ and $\hat{q}^y$ to have the property, up to fourth-order, that

$$\begin{aligned}\frac{\partial \hat{q}^x}{\partial x} =& q_x - u\frac{\Delta t}{2!}q_{xx} - v\frac{\Delta t}{2!}q_{xy} + u^2\frac{\Delta t^2}{3!}q_{xxx} + uv\frac{\Delta t^2}{4}q_{xxy} + v^2\frac{\Delta t^2}{4}q_{xyy} \\ & - u^3\frac{\Delta t^3}{4!}q_{xxxx} - u^2v\frac{2\Delta t^3}{4!}q_{xxxy} - uv^2\frac{3\Delta t^3}{4!}q_{xxyy} - v^3\frac{2\Delta t^3}{4!}q_{xyyy}\end{aligned} \tag{12}$$

and

$$\begin{aligned}\frac{\partial \hat{q}^y}{\partial y} =& q_y - u\frac{\Delta t}{2!}q_{xy} - v\frac{\Delta t}{2!}q_{yy} + u^2\frac{\Delta t^2}{4}q_{xxy} + uv\frac{\Delta t^2}{4}q_{xyy} + v^2\frac{\Delta t^2}{3!}q_{yyy} \\ & - u^3\frac{2\Delta t^3}{4!}q_{xxxy} - u^2v\frac{3\Delta t^3}{4!}q_{xxyy} - uv^2\frac{2\Delta t^3}{4!}q_{xyyy} - v^3\frac{\Delta t^3}{4!}q_{yyyy}\end{aligned} \tag{13}$$

Therefore, to capture this property, $\hat{q}^x$ and $\hat{q}^y$ up to fourth-order could have the form

$$\begin{aligned}\hat{q}^x_{\text{full}} =& q - u\frac{\Delta t}{2!}q_x - v\frac{\Delta t}{2!}q_y + u^2\frac{\Delta t^2}{3!}q_{xx} + uv\frac{\Delta t^2}{4}q_{xy} + v^2\frac{\Delta t^2}{4}q_{yy} \\ & - u^3\frac{\Delta t^3}{4!}q_{xxx} - u^2v\frac{2\Delta t^3}{4!}q_{xxy} - uv^2\frac{3\Delta t^3}{4!}q_{xyy} - v^3\frac{2\Delta t^3}{4!}q_{yyy}\end{aligned} \tag{14}$$

and

$$\begin{aligned}\hat{q}^y_{\text{full}} =& q - u\frac{\Delta t}{2!}q_x - v\frac{\Delta t}{2!}q_y + u^2\frac{\Delta t^2}{4}q_{xx} + uv\frac{\Delta t^2}{4}q_{xy} + v^2\frac{\Delta t^2}{3!}q_{yy} \\ & - u^3\frac{2\Delta t^3}{4!}q_{xxx} - u^2v\frac{3\Delta t^3}{4!}q_{xxy} - uv^2\frac{2\Delta t^3}{4!}q_{xyy} - v^3\frac{\Delta t^3}{4!}q_{yyy}\end{aligned} \tag{15}$$

The forms of $\hat{q}^x$ and $\hat{q}^y$ derived here are the standard $\hat{q}^x$ and $\hat{q}^y$ for forward-in-time schemes, in this paper we call them the full flux term formulation (hence the subscript 'full'), and can be discretized using standard finite-differences. This starting point allows us to create flux-form advection schemes with high order spatial and temporal accuracy, as this form of $\hat{q}^x$ and $\hat{q}^y$ can also be used in the flux form discretization (11). This can be extended to give arbitrary order (although we only show up to fourth-order in equations (14)-(15)).

The multi-dimensional forward-in-time schemes calculate each term in the fluxes $F = u\hat{q}^x$ and $G = v\hat{q}^y$ from (14) and (15) up to the desired order, and this method captures all of the cross-terms. The second-order version is the well known Lax-Wendroff scheme. The third-order version has been used by [LeVeque(1996)] and [Leonard et al.(1993)] (called the UTOPIA scheme). The discretization of $\hat{q}^x$ and $\hat{q}^y$ for the second and fourth-order schemes using finite-difference approximations is given in A and B.

## 3. THE ASYMMETRIZED FLUX FORMULATION

To increase the efficiency of the advection schemes it is desirable to reduce the number of terms in $\hat{q}^x$ and $\hat{q}^y$. As we increase to higher-order, not only are there more terms in the fluxes, but each term will generally require a larger stencil when discretized. For example, to fourth-order both (14) and (15) contain 10 terms each. One method to reduce computational cost would be to replace the full

flux terms with strictly one-dimensional flux terms, e.g.

$$\hat{q}^x_{\text{one}} = q - u\frac{\Delta t}{2!}q_x + u^2\frac{\Delta t^2}{3!}q_{xx} - u^3\frac{\Delta t^3}{4!}q_{xxx} + ... \tag{16}$$

$$\hat{q}^y\text{one} = q - v\frac{\Delta t}{2!}q_y + v^2\frac{\Delta t^2}{3!}q_{yy} - v^3\frac{\Delta t^3}{4!}q_{yyy} + ... \tag{17}$$

However, this method then neglects the cross-terms in (9), which can lead to a reduction in accuracy and to instabilities for two-dimensional flow [Leonard et al.(1996)].

Here we introduce a method that reduces the number of terms in one flux, for example in $\hat{q}^y$, and replaces them in the other, $\hat{q}^x$. We first demonstrate how this is achieved for second-order, before moving up to fourth-order. Consider the second-order expansion (8). Note the $\Delta t^2 uvq_{xy}$ term. In the formulation of $\hat{q}^x$ and $\hat{q}^y$, up to second-order in (14) and (15), this term is calculated using the $q_y$ term in $\hat{q}^x$, and the $q_x$ term in $\hat{q}^y$. Therefore this cross-term is produced by terms from both $\hat{q}^x$ and $\hat{q}^y$. To improve efficiency we can remove the $q_x$ term from $\hat{q}^y$, and add a corresponding $q_y$ term to $\hat{q}^x$:

$$\hat{q}^x_{\text{afc}} = q - u\frac{\Delta t}{2!}q_x - v\Delta t q_y, \tag{18}$$

$$\hat{q}^y_{\text{afc}} = q - v\frac{\Delta t}{2!}q_y. \tag{19}$$

Using $\hat{q}^x$ and $\hat{q}^y$ in (10) will produce approximations of all the terms in (8), but they contain one fewer term in the calculation of $\hat{q}^y$. We call this form of $\hat{q}^x$ and $\hat{q}^y$ the *asymmetrized flux calculation*. For the higher-order forward-in-time schemes we can remove more terms from one flux and stack them on the other. Up to fourth-order we have

$$\begin{aligned}\hat{q}^x_{\text{afc}} =& q - u\frac{\Delta t}{2!}q_x - v\Delta t q_y + u^2\frac{\Delta t^2}{3!}q_{xx} + uv\frac{\Delta t^2}{2}q_{xy} + v^2\frac{\Delta t^2}{2}q_{yy} \\ &- u^3\frac{\Delta t^3}{4!}q_{xxx} - u^2 v\frac{4\Delta t^3}{4!}q_{xxy} - uv^2\frac{6\Delta t^3}{4!}q_{xyy} - v^3\frac{4\Delta t^3}{4!}q_{yyy}\end{aligned} \tag{20}$$

$$\hat{q}^y_{\text{afc}} = q - v\frac{\Delta t}{2!}q_y + v^2\frac{\Delta t^2}{3!}q_{yy} - v^3\frac{\Delta t^3}{4!}q_{yyy} \tag{21}$$

For second-order only terms up to $\Delta t$ are required, and for third-order only terms up to $\Delta t^2$. The terms in $\hat{q}^x$ and $\hat{q}^y$ given here can be discretized in a number of ways. The discretization of the asymmetrized flux calculation using finite-difference approximations is given in A and B for the second and fourth-order scheme respectively.

The benefit of the asymmetrized flux calculation is the reduction in the number of terms, and hence the reduction in computational cost when compared with the full fluxes, whilst retaining the formal order-of-accuracy. The second, third, and fourth-order asymmetrized flux calculations of $\hat{q}^x$ and $\hat{q}^y$ contain 1, 3, and 6 fewer terms than the full formulation given in (14)-(15). The reduction in cost is shown in A for the second-order discretization. It is shown that the total number of operations for the full flux terms is 20, whereas the asymmetrized flux terms only require 15 operations. This indicates that the second-order full $\hat{q}^x$ and $\hat{q}^y$ are approximately $33\%$ more expensive than the asymmetrized flux calculation. The total number of operations is computed for the fourth-order discretization in B, and this shows that the fourth-order full $\hat{q}^x$ and $\hat{q}^y$ are approximately $59\%$ more expensive than the fourth-order asymmetrized flux calculation.

Stability analysis can be applied to the full and asymmetrized flux formulations using the discretizations given in the appendix. We let $c_x = u\Delta t/\Delta x$ and $c_y = v\Delta t/\Delta y$ denoted the Courant numbers in the x and y directions respectively. From [Turkel(1977)] it can be shown that the full second-order method is stable provided $c_x^{2/3} + c_y^{2/3} \leq 1$, and from [Thuburn(1996)] it is shown that the full third-order method is stable for $|c_x| + |c_y| \leq 1$. The stability of the asymmetrized flux formulations can be numerically calculated for varying Courant numbers. For each scheme, for each Courant number, the amplitude factor is computed. If the magnitude of the amplitude factor exceeds

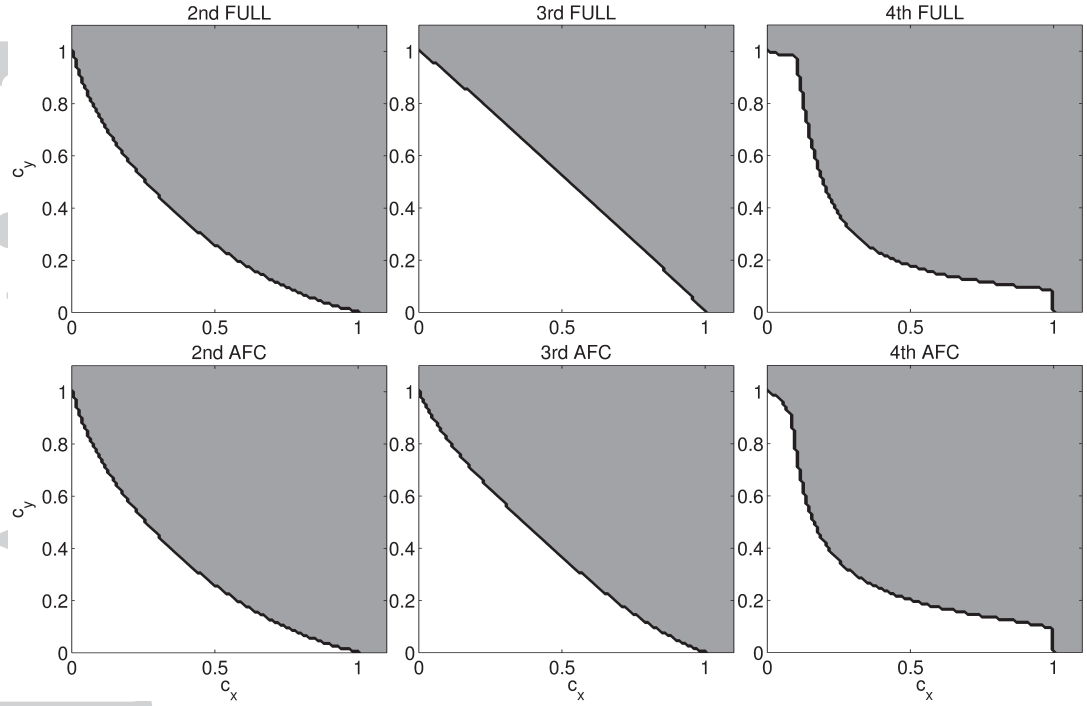


Figure 1. The stability of the second, third, and fourth-order schemes for the full fluxes (top) and the asymmetrized fluxes (bottom), for varying Courant numbers. White indicates the stable region, and grey indicates the unstable region.

1 for any wave number, then the scheme is classed as unstable at those $c_x$ and $c_y$ values. The stability regions of the second, third, and fourth-order schemes using the full fluxes and the asymmetrized flux calculation are shown in Figure 1. This plot shows that the stability region of the asymmetrized flux calculation schemes are very similar to the corresponding full schemes.

However, the stability criteria can be improved by using an upwind discretization on the cross terms [Durran(2010)]. The upwinding of the cross terms relaxes the stability criteria to

$$0 \leq \frac{u\Delta t}{\Delta x} \leq 1, \qquad \text{and} \qquad 0 \leq \frac{v\Delta t}{\Delta y} \leq 1. \tag{22}$$

To achieve the improved stability criteria for the asymmetrized flux formulation, the upwinding of the cross terms only takes place in $\hat{q}^x$.

A final consideration for these advection schemes is the use of monotonic and positivity-preserving limiters. For the forward-in-time schemes discretized in the appendix, in both full and asymmetrized flux form, flux-limiters are easily applied. It is possible to just apply one-dimensional limiters, for example the universal limiter [Leonard(1991)], in each coordinate direction. However, for forward-in-time advection schemes a one-dimensional limiter does not properly limit the cross-terms, and therefore even the use of a monotonic one-dimensional limiter will not guarantee monotonicity for multidimensional flow. Applying a fully monotonic multidimensional limiter (e.g. [Thuburn(1996)]) to $\hat{q}^x$ and $\hat{q}^y$ ensures monotonicity.

## 4. TWO-DIMENSIONAL NUMERICAL TESTING

The aim of the numerical testing is to demonstrate that the asymmetrized flux calculation has the same accuracy as the full formulation (for corresponding order-of-accuracy) but with reduced computational cost. To show the accuracy and efficiency of the asymmetrized flux calculation forward-in-time scheme we perform a variety of idealized tests. We calculate normalized error

norms, convergence rates, and the run time taken to complete the simulation. The average time taken from three runs is used. Note that the tests are performed on a desktop computer and therefore the timings are used only for comparison within this paper. In each test we use the flux-form of the discretizations, equation (11), with constant density, $\rho = 1$. The grid is doubly periodic with $0 < x \leq 1$, $0 < y \leq 1$. For these tests no upwinding is used on the cross-terms in any of the discretizations. Note that in practice the third-order schemes use upwinding to calculate several of the terms to third-order accuracy, and the stencil depends on the sign of the velocity. For the testing used here the velocities are always positive.

We test the forward-in-time schemes of order $2-4$ (with the discretizations given in the appendix) with the full flux (denoted FULL), e.g. explicitly calculating each term in equations (14) and (15), in asymmetrized flux calculation form (AFC), e.g. using the method described in Section 3, and finally the formulation with only the one-dimensional flux (ONE), e.g. (16) and (17).

### *4.1. Constant Velocities*

The first test advects a smooth tracer using constant velocities. We use the initial conditions

$$u = 1, \qquad v = 1, \qquad q_1 = \exp\left(-50\left[\frac{1}{2} - x\right]^2 - 50\left[\frac{1}{2} - y\right]^2\right) \tag{23}$$

The tracer is advected once around the domain and back to its starting point to allow the easy calculation of error norms. Using a time step of $\Delta t = 1/1280$ we calculate the normalized $\ell_2$ error norms for each scheme on the grid with $128$ grid points in both directions. Using a time step of $\Delta t = \Delta x/5$ we calculate the error convergence rate [Holdaway et al.(2008)] by calculating the normalized $\ell_2$ error norms on grids with $64$ and $128,\ 256$ and $512$ grid points in both directions.

The results for the constant advection case are given in the left hand section of Table I. A dash is used to indicate that a scheme became unstable. The testing shows that the one-dimensional fluxes are the least accurate, don't converge at the formal rate, and can become unstable. This demonstrates the need to capture the cross-terms. For each order-of-accuracy the $\ell_2$ error norms are very similar for the full flux and the asymmetrized flux formulations, and both methods achieve the same empirical convergence rate. The error convergence rates are close to the formal order-of-accuracy for these schemes for constant velocities. This demonstrates that the accuracy of the asymmetrized flux calculation is comparable to the full flux method. The wall clock timings show that the asymmetrized fluxes are quicker than the full fluxes for each order (with the benefit increasing as the order increases). The asymmetrized flux calculation produces a solution in $91\%$, $80\%$, and $67\%$ of the time of the full flux formulation for second, third, and fourth order respectively. This agrees with the cost analysis shown in A.

Table I. Normalized $\ell_2$ error norms for $q_1$ for each of the schemes for $u = v = 1$. The grid is composed of $128$ grid points in each direction. Also shown is the mean clock time of the simulation (for the $128$ grid), and the mean numerical convergence rate for $q_1$ with $u = v = 1$ when using $64,\ 128,\ 256$ and $512$ grid points. The right hand section shows the metrics for $q_2$ for the deformational flow, and here the normalized $\ell_2$ error norms are for the $128$ grid point grid. A dash indicates that the scheme became unstable.

| **Order** | **Scheme** | $q_1$ $\ell_2$ | time (s) | Rate | $q_2$ $\ell_2$ | Rate |
|---|---|---|---|---|---|---|
| 2nd | FULL | $1.93 \times 10^{-2}$ | 0.61 | 1.99 | $4.79 \times 10^{-2}$ | 1.88 |
| 2nd | ONE | $4.38 \times 10^{-2}$ | 0.40 | 1.17 | 0.65 | 1.87 |
| 2nd | AFC | $1.93 \times 10^{-2}$ | 0.56 | 1.99 | $4.80 \times 10^{-2}$ | 1.88 |
| 3rd | FULL | $1.40 \times 10^{-3}$ | 1.53 | 2.98 | $4.69 \times 10^{-3}$ | 2.75 |
| 3rd | ONE | $3.91 \times 10^{-2}$ | 0.59 | 1.00 | 0.11 | 1.75 |
| 3rd | AFC | $1.40 \times 10^{-3}$ | 1.22 | 2.98 | $5.47 \times 10^{-3}$ | 2.75 |
| 4th | FULL | $9.96 \times 10^{-5}$ | 3.59 | 3.69 | $6.02 \times 10^{-4}$ | 3.81 |
| 4th | ONE | $3.92 \times 10^{-2}$ | 0.98 | - | - | 1.09 |
| 4th | AFC | $1.01 \times 10^{-4}$ | 2.41 | 3.66 | $2.84 \times 10^{-3}$ | 3.66 |

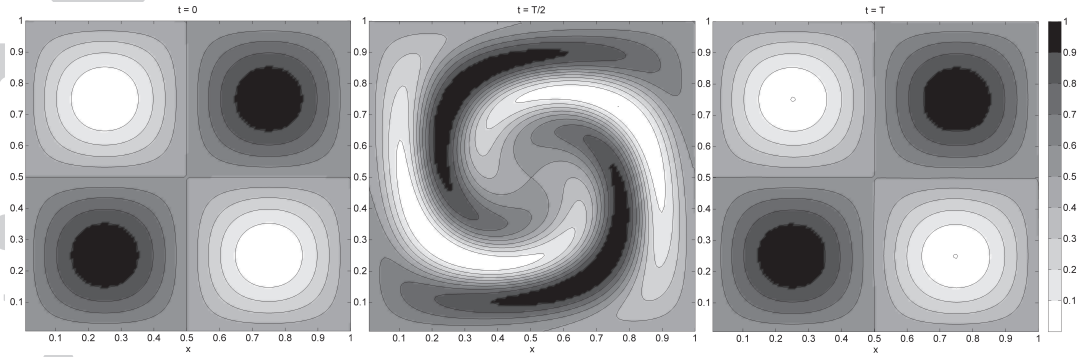


Figure 2. The evolution of tracer $q_2$ for the deformation test using the fourth order asymmetrized flux calculation on the $128 \times 128$ grid, at time 0 (left), time $T/2$ (centre), and time $T$ (right).

### *4.2. Deformational Flow*

We now run the schemes using a deformational flow that has a time dependent term that returns the tracers to their initial conditions. Added to the deformational velocities is a constant background flow. The translated $x$ and $y$ coordinates are given as

$$x' = x - v_0 \frac{t}{T}, \qquad y' = y - v_0 \frac{t}{T}, \tag{24}$$

and the deformational velocities are given as

$$u = u_0 \sin^2 \pi x' \sin 2\pi y' \cos \frac{\pi t}{T} + v_0, \qquad v = -u_0 \sin^2 \pi y' \sin 2\pi x' \cos \frac{\pi t}{T} + v_0. \tag{25}$$

Here $T$ is the total length of the simulation, in this case $T = 1$, the magnitude of the deformation velocity is given by $u_0 = 2$, and the background velocity is $v_0 = 2$. Note that the flow is non-divergent, $u_x + v_y = 0$, and so the advective and flux forms of the equations are equivalent. The initial tracer is given as

$$q_2 = \frac{1}{2} + \frac{1}{2} \sin(2\pi x) \sin(2\pi y) . \tag{26}$$

As with the constant case, the initial tracer can be used as the true solution, and therefore error norms can be calculated. We use a grid of $128$ grid points in both directions, and a time step of $1/1280$. The empirical error convergence rates are computed using the normalized $\ell_2$ errors on the grids with $64$ and $128$ grid points. The time step used for these convergence simulations is $\Delta t = \Delta x/100$.

The results for the deformation test are given in the right hand section of Table I, and the tracer evolution using the fourth order asymmetrized flux calculation is shown in Figure 2. For the second and fourth-order schemes, the one-dimensional fluxes become unstable, showing their unsuitability for capturing the cross terms. As with the constant velocity case, the normalized $\ell_2$ error norms are similar for both the full fluxes and asymmetrized fluxes for both second- and third-order. However, there is a difference in the error norm for the fourth-order schemes, with the full fluxes producing a smaller error. This is due to the velocities for the cross-terms in the asymmetrized flux only being stored at one flux point. The asymmetrized flux calculation has similar error convergence rates as the corresponding full formulation. These results demonstrate that although there are more pronounced differences for non-constant velocities, both the asymmetrized flux calculation and full formulation perform to a similar level of accuracy.

### *4.3. Use with Limiters*

We can use the one-dimensional universal limiter of [Leonard(1991)] and the two-dimensional version of [Thuburn(1996)] to show the effect of limiters on these schemes. Using the constant velocities on the $64 \times 64$ grid, with a time step $\Delta t = 1/640$, we repeat the test using a discontinuous

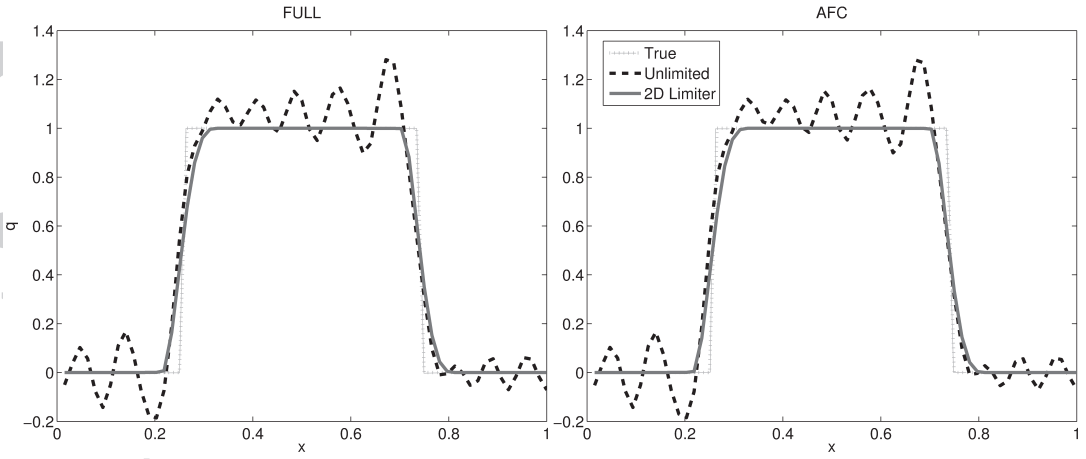


Figure 3. Cross-section of $q_3$ at the end of the simulation for the full fluxes (left) and the asymmetrized flux calculation (right) using the fourth-order scheme at $y = 1/2$. Shown in each plot are the true solution, the unlimited fourth-order scheme, and the fourth-order scheme with the 2D limiter of [Thuburn(1996)].

initial tracer given by $q_3 = 1$ if $|x - 0.5| < 0.25$ and $|y - 0.5| < 0.25$, and $q_3 = 0$ otherwise. For each case we calculate the $\ell_2$ error norm and the minimum value of $q$ at the end of the simulation. The analytical minimum is zero. Error convergence rates are not computed for this test due to the discontinuous initial data [Holdaway et al.(2008)].

The results, shown in Table II, generally agree with those given in Table I. As before, the asymmetrized flux calculation and the full fluxes produce similar error norms, and this holds when the flux limiters are applied. The one-dimensional flux-like terms, which can be unstable for the unlimited case, perform better with the addition of the limiters, although the error norms are still larger than the full and asymmetrized flux formulation. The results also show that each of the unlimited schemes are not monotonic, with the third-order scheme producing the smallest magnitude undershoots. Using the one-dimensional limiter reduces the magnitude of the undershoots, but the cross-terms are unlimited and so each scheme is still not monotonic. Applying the two-dimensional limiter improves the error norms for this test, and is the only method shown that makes each of the schemes monotonic. A cross-section at the end of the simulation of $q_3$ at $y = 1/2$ is shown in Figure 3 for the full and asymmetrized flux formulations of the fourth-order scheme with and without the limiter of [Thuburn(1996)]. This plot highlights that the asymmetrized flux calculation produces very similar results to those of the full formulation even when monotonic limiters are applied.

Table II. Normalized $\ell_2$ error norms for $q_3$ on the $64 \times 64$ grid for each of the schemes with and without the limiters for $u = v = 1$. Also shown is the minimum value for each scheme (the true value is 0)

| | | Unlimited | | 1D Limiter | | 2D Limiter | |
|---|---|---|---|---|---|---|---|
| **Order** | **Scheme** | $\ell_2$ | min | $\ell_2$ | min | $\ell_2$ | min |
| 2nd | FULL | 0.37 | -0.37 | 0.29 | $-2.68 \times 10^{-2}$ | 0.28 | 0 |
| 2nd | ONE | - | - | 0.29 | $-2.68 \times 10^{-2}$ | 0.30 | 0 |
| 2nd | AFC | 0.37 | -0.37 | 0.29 | $-4.23 \times 10^{-2}$ | 0.28 | 0 |
| 3rd | FULL | 0.25 | -0.12 | 0.26 | $-3.00 \times 10^{-3}$ | 0.25 | 0 |
| 3rd | ONE | 0.79 | -1.84 | 0.27 | $-4.05 \times 10^{-1}$ | 0.27 | 0 |
| 3rd | AFC | 0.25 | -0.13 | 0.27 | $-1.06 \times 10^{-2}$ | 0.25 | 0 |
| 4th | FULL | 0.30 | -0.33 | 0.23 | $-5.67 \times 10^{-2}$ | 0.20 | 0 |
| 4th | ONE | - | - | 0.35 | -1.13 | 0.32 | 0 |
| 4th | AFC | 0.30 | -0.34 | 0.24 | $-8.47 \times 10^{-2}$ | 0.20 | 0 |

## 5. EXTENSION TO THREE-DIMENSIONAL FLOW

The method described in this paper can easily be extended to three dimensions. The advection equation in three-dimensions becomes

$$q_t + uq_x + vq_y + wq_z = 0, \tag{27}$$

where $w$ is the velocity in the $z$ direction. The forward-in-time method can be derived once more using Taylor series expansions. The Taylor expansion of the advection equation is given as

$$q_{ijk}^{n+1} = q_{ijk} + \Delta t q_t + \frac{\Delta t^2}{2!}q_{tt} + \frac{\Delta t^3}{3!}q_{ttt} + \frac{\Delta t^4}{4!}q_{tttt} + ... \tag{28}$$

where $k$ is the spatial index in the $z$ direction and the derivatives are evaluated at the point $i, j, k$. Considering the case of constant velocities, we use the same method as before to substitute expressions for spatial derivatives into higher order temporal derivatives. Substituting these higher derivatives into the Taylor expansion (28) gives (to fourth-order)

$$\begin{aligned} q_{ij}^{n+1} = q_{ij}^n - \Delta t\left(uq_x + vq_y + wq_z\right) + \frac{\Delta t^2}{2!}\left(u^2q_{xx} + v^2q_{yy} + w^2q_{zz} + 2uvq_{xy} + 2uwq_{xz} + 2vwq_{yz}\right) \\ - \frac{\Delta t^3}{3!}\Big(u^3q_{xxx}+v^3q_{yyy}+w^3q_{zzz}+6uvwq_{xyz}+3u^2vq_{xxy}+3u^2wq_{xxz}+3uv^2q_{xyy}+3uw^2q_{xzz}+3v^2wq_{yyz}+3vw^2q_{yzz}\Big) \\ + \frac{\Delta t^4}{4!}\Big(u^4q_{xxxx}+v^4q_{yyyy}+w^4q_{zzzz}+4u^3vq_{xxxy}+6u^2v^2q_{xxyy}+4uv^3q_{xyyy}+4u^3wq_{xxxz}+6u^2w^2q_{xxzz} \\ +4uw^3q_{xzzz}+4v^3wq_{yyyz}+6v^2w^2q_{yyzz}+4vw^3q_{yzzz}+12u^2vwq_{xxyz}+12uv^2wq_{xyyz}+12uvw^2q_{xyzz}\Big) \end{aligned} \tag{29}$$

As with the two-dimensional case, the values of $q$ at the grid cell edges ($\hat{q}^x$, $\hat{q}^y$ and $\hat{q}^z$) can be calculated such that

$$q_{ijk}^{n+1} = q_{ijk}^n - u\frac{\Delta t}{\Delta x}\left(\hat{q}^x_{i+\frac{1}{2}jk} - \hat{q}^x_{i-\frac{1}{2}jk}\right) - v\frac{\Delta t}{\Delta y}\left(\hat{q}^y_{ij+\frac{1}{2}k} - \hat{q}^y_{ij-\frac{1}{2}k}\right) - w\frac{\Delta t}{\Delta z}\left(\hat{q}^z_{ijk+\frac{1}{2}} - \hat{q}^z_{ijk-\frac{1}{2}}\right). \tag{30}$$

Therefore the full formulation of $\hat{q}^x$, $\hat{q}^y$ and $\hat{q}^z$, to fourth-order, is

$$\begin{aligned} \hat{q}^x_{\text{full}} = q - u\frac{\Delta t}{2!}q_x - v\frac{\Delta t}{2!}q_y - w\frac{\Delta t}{2!}q_z + \frac{\Delta t^2}{6}\left(u^2q_{xx} + \frac{3}{2}uvq_{xy} + \frac{3}{2}v^2q_{yy} + \frac{3}{2}uwq_{xz} + 2vwq_{yz} + \frac{3}{2}w^2q_{zz}\right) \\ - \frac{\Delta t^3}{24}\Big(u^3q_{xxx}+2u^2vq_{xxy}+3uv^2q_{xyy}+2v^3q_{yyy}+2u^2wq_{xxz}+3uw^2q_{xzz}+2w^3q_{zzz}+4v^2wq_{yyz}+4vw^2q_{yzz}+4uvwq_{xyz}\Big), \end{aligned} \tag{31}$$

$$\begin{aligned} \hat{q}^y_{\text{full}} = q - u\frac{\Delta t}{2!}q_x - v\frac{\Delta t}{2!}q_y - w\frac{\Delta t}{2!}q_z + \frac{\Delta t^2}{6}\left(\frac{3}{2}u^2q_{xx} + \frac{3}{2}uvq_{xy} + v^2q_{yy} + 2uwq_{xz} + \frac{3}{2}vwq_{yz} + \frac{3}{2}w^2q_{zz}\right) \\ - \frac{\Delta t^3}{24}\Big(v^3q_{yyy}+2u^3q_{xxx}+3u^2vq_{xxy}+2uv^2q_{xyy}+2v^2wq_{yyz}+3vw^2q_{yzz}+2w^3q_{zzz}+4u^2wq_{xxz}+4uw^2q_{xzz}+4uvwq_{xyz}\Big), \end{aligned} \tag{32}$$

and

$$\begin{aligned} \hat{q}^z_{\text{full}} = q - u\frac{\Delta t}{2!}q_x - v\frac{\Delta t}{2!}q_y - w\frac{\Delta t}{2!}q_z + \frac{\Delta t^2}{6}\left(\frac{3}{2}u^2q_{xx} + 2uvq_{xy} + \frac{3}{2}v^2q_{yy} + \frac{3}{2}uwq_{xz} + \frac{3}{2}vwq_{yz} + w^2q_{zz}\right) \\ - \frac{\Delta t^3}{24}\Big(w^3q_{zzz}+2u^3q_{xxx}+3u^2wq_{xxz}+2uw^2q_{xzz}+2v^3q_{yyy}+3v^2wq_{yyz}+2vw^2q_{yzz}+4u^2vq_{xxy}+4uv^2q_{xyy}+4uvwq_{xyz}\Big). \end{aligned} \tag{33}$$

We can use the same method as before to write the flux terms using the asymmetrized flux calculation. The fourth-order asymmetrized flux formula for three-dimensional flow becomes

$$\hat{q}^x_{\text{afc}} = q - u\frac{\Delta t}{2!}q_x - v\Delta t q_y - w\Delta t q_z + \frac{\Delta t^2}{6}\left(u^2 q_{xx} + 3uvq_{xy} + 3v^2 q_{yy} + 3uwq_{xz} + 6vwq_{yz} + 3w^2 q_{zz}\right) \tag{34}$$

$$-\frac{\Delta t^3}{24}\left(u^3 q_{xxx} + 4u^2 v q_{xxy} + 6uv^2 q_{xyy} + 4v^3 q_{yyy} + 4u^2 w q_{xxz} + 6uw^2 q_{xzz} + 4w^3 q_{zzz} + 12v^2 w q_{yyz} + 12vw^2 q_{yzz} + 12uvw q_{xyz}\right)$$

$$\hat{q}^y_{\text{afc}} = q - v\frac{\Delta t}{2!}q_y - w\Delta t q_z + \frac{\Delta t^2}{6}\left(v^2 q_{yy} + 3vwq_{yz} + 3w^2 q_{zz}\right) - \frac{\Delta t^3}{24}\left(v^3 q_{yyy} + 4v^2 w q_{yyz} + 6vw^2 q_{yzz} + 4w^3 q_{zzz}\right), \tag{35}$$

$$\hat{q}^z_{\text{afc}} = q - w\frac{\Delta t}{2!}q_z + \frac{\Delta t^2}{6}w^2 q_{zz} - \frac{\Delta t^3}{24}w^3 q_{zzz}. \tag{36}$$

As an efficiency calculation, the fourth-order asymmetrized fluxes have a total of $34$ terms instead of the $60$ terms for the full flux-like terms in equations (31)-(33). For second-order the asymmetrized flux formulation has $9$ terms compared to $12$ in the full formulation, and the third-order asymmetrized flux calculation has $19$ terms compared to $30$ in the full formulation. The second-order discretization is shown in A, and here the number of operations is calculated to compare computational efficiency. The full fluxes require a total of $42$ operations compared to $27$ for the asymmetrized flux calculation, indicating that for three-dimensional flow the second-order full fluxes are approximately $56\%$ more expensive than the asymmetrized fluxes. Note that in the asymmetrized flux calculation, $H$ is strictly one-dimensional, $G$ is two-dimensional, and $F$ is three-dimensional.

### *5.1. 3D Testing*

The constant velocities test is extended to three-dimensions. The grid is triply periodic with $0 < x \leq 1, 0 < y \leq 1, 0 < z \leq 1$, and the initial conditions are

$$u = 1, \qquad v = 1, \qquad w = 1, \qquad q_4 = \exp\left(-50\left[\frac{1}{2} - x\right]^2 - 50\left[\frac{1}{2} - y\right]^2 - 50\left[\frac{1}{2} - z\right]^2\right). \tag{37}$$

For the three-dimensional schemes we test the full flux (FULL), from equations (31)-(33), the asymmetrized flux calculation (AFC), from equations (34)-(36), and the one-dimensional flux (ONE) that capture no cross-terms (i.e. $\hat{q}^x$, $\hat{q}^y$ and $\hat{q}^z$ are strictly one-dimensional). For this test no limiters are used. The grid is made up of $64$ grid points in each direction, and the time step is $\Delta t = 1/640$.

The results for the three-dimensional test are presented in Table III. The one-dimensional flux-like terms have the lowest computational cost but the largest error norms (and for an increased time step become unstable). The results are similar to the two-dimensional tests, as for each order-of-accuracy the full formulation and the asymmetrized flux calculation produce similar sized error norms, yet the run time for the asymmetrized flux calculation is less than that of the full scheme. This is especially notable for higher than second-order, and agrees with the cost analysis performed in A.

## 6. CONCLUSIONS

Accurate and efficient advection schemes are required in all branches of computational fluid dynamics. This is especially true for numerical models of the atmosphere, where advection schemes are used for tracer transport. For multi-dimensional flow it is essential that forward-in-time schemes adequately capture the cross-terms. We have provided a method to reduce the number of terms in the fluxes of forward-in-time advection schemes. Duplicated terms are removed from one flux and loaded onto the other, to create an asymmetrized flux. Although symmetry might be a desirable property of an advection scheme, the testing in this paper shows that the asymmetrized flux

Table III. Normalized $\ell_2$ error norms for $q_4$ for each of the schemes for $u = v = w = 1$. The grid is composed of $64$ grid points in each direction. Also shown is the clock time of the simulation.

| **Order** | **Scheme** | $q_4$ $\ell_2$ | time (s) |
|---|---|---|---|
| 2nd | FULL | $7.65 \times 10^{-2}$ | 12.6 |
| 2nd | ONE | $1.12 \times 10^{-1}$ | 5.8 |
| 2nd | AFC | $7.65 \times 10^{-2}$ | 11.5 |
| 3rd | FULL | $1.08 \times 10^{-2}$ | 44.2 |
| 3rd | ONE | $7.76 \times 10^{-2}$ | 8.1 |
| 3rd | AFC | $1.08 \times 10^{-2}$ | 28.5 |
| 4th | FULL | $1.51 \times 10^{-3}$ | 119.8 |
| 4th | ONE | $7.94 \times 10^{-2}$ | 12.8 |
| 4th | AFC | $1.51 \times 10^{-3}$ | 77.0 |

calculation performs to the same degree of accuracy as the full, symmetric, flux formulation. For the asymmetrized flux calculation for the two-dimensional case, the second-order version results in a reduction from $6$ terms to $5$ terms, for third-order it is a reduction from $12$ to $9$ terms, and for fourth-order it is a reduction from $20$ to $14$ terms. This reduction in the number of terms reduces the computational cost of the asymmetrized flux calculation when compared to the full formulation. Further cost analysis shows that for second-order, the number of operations required for the full fluxes is $20$, whereas it is only $15$ for the asymmetrized flux. This means that the full fluxes are $\approx 33\%$ more expensive than the asymmetrized flux calculation. Increasing the order-of-accuracy to fourth order we find that the full fluxes are $\approx 59\%$ more expensive than the asymmetrized flux calculation. As the order-of-accuracy increases further, the full flux formulation becomes even more expensive than the asymmetrized flux calculation. The asymmetrized flux calculation is easily extendible to three-dimensional flow, and in this case the reduction in computational time is more pronounced.

Numerical testing highlights the importance of capturing the cross terms, with the strictly one-dimensional schemes producing the largest errors, and in some cases instabilities. The results from the numerical testing show that for constant velocity transport problems the error norms and error convergence rates are almost identical between same order schemes with the full formulation and asymmetrized flux calculation. This demonstrates that using the asymmetrized flux calculation results in no loss of accuracy when compared to the full formulation. However, the asymmetrized flux calculation offers a noticeable reduction in computational time, completing the constant velocity simulation in $67\%$ of the time of the full formulation for the fourth-order method. For the non-constant velocity deformational tests, the error norms are slightly larger for the asymmetrized flux calculation, and this is due to the location of the velocities used to calculate the cross-terms in the fluxes.

The discretizations of the schemes in this paper make use of finite-difference approximations which are not monotonic. Limiters, such as that of [Thuburn(1996)], can be easily applied to the methods shown here. One-dimensional flux limiters fail to make the schemes completely monotonic because the cross-terms are not limited, whereas fully multidimensional limiters properly limit the cross-terms and produce a monotonic solution.

The aim of this article is to introduce the asymmetrized flux calculation concept, and as such the analysis and testing has been performed on a Cartesian domain using a structured grid for advection problems. Future studies will show the application of the asymmetrized flux calculation on unstructured and distorted grids, and for other equation sets.

ACKNOWLEDGEMENTS

The author would like to thank Nigel Wood, Ben Shipway, and Stephen Pring (all Met Office) for many useful discussions about this topic. The author would also like to thank three anonymous reviewers for their comments which greatly improved the manuscript.

REFERENCES

Abgrall, R. 2001. Toward the Ultimate Conservative Scheme: Following the Quest. *J. Comput. Phys.*, **1670**, 277-315.

Bosler, P. A., Kent, J., Krasny, R., and Jablonowski, C. 2017. A Lagrangian Particle Method for Tracer Transport on the Sphere. *J. Comput. Phys.*, **340**, 639-654.

Crowley, W. P. 1968. Numerical Advection Experiments. *Mon. Weather Rev.*, **96**, 1-11.

Durran, D. R. 2010. Numerical Methods for Fluid Dynamics. *Springer*, pp 516.

Holdaway, D., Thuburn, J., and Wood, N. 2008. On the relation between order of accuracy, convergence rate and spectral slope for linear numerical methods applied to multiscale problems. *Int. J. Numer. Meth. Fluids*, **56**, 1297-1303.

Katta, K. K., Nair, R. D., and Kumar, V. 2015. High-Order Finite-Volume Transport on the Cubed Sphere: Comparison between 1D and 2D Reconstruction Schemes. *Mon. Weather Rev.*, **143**, 2937-2954.

Lamine, S. and Edwards, M. G. 2013. Higher order cell-based multidimensional upwind schemes for flow in porous media on unstructured grids. *Comput. Methods Appl. Mech. Engrg.*, **256**, 103-122.

Lauritzen, P. H., Ullrich, P. A., and Nair, R. D. 2011. Atmospheric Transport Schemes: desirable properties and a semi-Lagrangian view on finite-volume discretizations, in Numerical Techniques for Global Atmospheric Models, eds. Lauritzen, P. H., Jablonowski, C., Taylor, M. A., and Nair, R. D. *Springer*, 187-254.

Lax, P. D. and Wendroff, B. 1960. Systems of conservation laws. *Commun. Pure Appl. Math.*, **13**, 217-237.

Leonard, B. P. 1991. The ULTIMATE conservative difference scheme applied to unsteady one-dimensional advection. *Comp. Methods. Applied. Mech. Eng.*, **88**, 17-74.

Leonard, B. P., MacVean, M. K. and Lock, A. P. 1993. Positivity-Preserving Numerical Schemes for Multidimensional Advection. *NASA Technical Memorandum 106055.*

Leonard, B. P., Lock, A. P., and MacVean, M. K. 1996. Conservative Explicit Unrestricted-Time-Step Multidimensional Constancy-Preserving Advection Schemes. *Mon. Weather Rev.*, **124**, 2588-2606.

LeVeque, R. 1996. High-Resolution Conservative Algorithms for Advection in Incompressible Flow. *SIAM J. Numer. Anal.*, 627-665.

Lin, S. J. and Rood, R. B. 1996. Multidimensional Flux-Form Semi-Lagrangian Transport Schemes. *Mon. Weather Rev.*, **124**, 2046-2070.

Lin, S. J. and Rood, R. B. 1997. An explicit flux-form semi-Lagrangian shallow water model on the Sphere, *Quart. J. Roy. Meteor. Soc.*, **123**, 2477-2498.

Melvin, T., Staniforth, A., Thuburn, J. 2012. Dispersion analysis of the spectral element method, *Quart. J. Roy. Meteor. Soc.*, **138**, 1934-1947.

Norman, M. R., Finkel, H. 2012. Multi-moment ADER-Taylor methods for systems of conservation laws with source terms in one dimension. *J. Comput. Phys.*, **231**, 6622-6642.

Rood, R. B. 1987. Numerical advection algorithms and their role in atmospheric transport and chemistry models. *Reviews of Geophysics*, **25**, 71-100.

Smolarkiewicz, P. K. 1982. The multidimensional Crowley advection scheme. *Mon. Weather Rev.*, **110**, 1968-1983.

Staniforth, A. and Côté, J. 1991. Semi-Lagrangian integration schemes for atmospheric models – A review. *Mon. Weather Rev.*, **119**, 2206-2223.

Thuburn, J. 1996. Multidimensional Flux-Limited Advection Schemes. *J. Comput. Phys.*, **123**, 74-83.

Toro, E. F., Millington, R. C., and Nejad, L. A. M. 2001. Towards Very High Order Godunov Schemes, in Godunov Methods: Theory and Applications, ed. Toro, E. F. *Kluwer Academic/Plenum Publishers*, 907-940.

Tremback, C. J., Powell, J., Cotton, W. R., and Pielke, R. A. 1987 The forward-in-time upstream advection scheme: extension to higher orders. *Mon. Weather Rev.*, **115**, 540-555.

Turkel, E., Symmetric Hyperbolic Difference Schemes and Matrix Problems, *Linear Algebra Appl.*, **16**, 109-129.

Zerroukat, M., Wood, N., and Staniforth, A. 2006. The Parabolic Spline Method (PSM) for conservative transport problems. *Int. J. Numer. Meth. Fluids*, **51**, 1297-1318.

## A. SECOND-ORDER DISCRETIZATIONS

### *A.1. Two-Dimensional Flow*

The discretizations in this appendix assume that $q$ is stored at integer grid points $(i, j)$, $F = u\hat{q}^x$ is stored at half $x$ points $(i \pm 1/2, j)$ and $G = v\hat{q}^y$ is stored at half $y$ points $(i, j \pm 1/2)$. For demonstrative purposes we will consider the case of constant $u$ and $v$, letting $C_x = u\Delta t/\Delta x$ and $C_y = v\Delta t/\Delta y$.

The **full fluxes** for the second-order scheme can be discretized using

$$\hat{q}^x_{i+\frac{1}{2}j} = \frac{1}{2}\left(q_{i+1j} + q_{ij}\right) - \frac{C_x}{2}\left(q_{i+1j} - q_{ij}\right) - \frac{C_y}{2}\left(q_{i+1/2j+1/2} - q_{i+1/2j-1/2}\right) \tag{38}$$

$$\hat{q}^y_{ij+\frac{1}{2}} = \frac{1}{2}\left(q_{ij+1} + q_{ij}\right) - \frac{C_x}{2}\left(q_{i+1/2j+1/2} - q_{i-1/2j+1/2}\right) - \frac{C_y}{2}\left(q_{ij+1} - q_{ij}\right) \tag{39}$$

where

$$q_{i+1/2j+1/2} = \frac{1}{4}\left(q_{ij} + q_{i+1j} + q_{ij+1} + q_{i+1j+1}\right) \tag{40}$$

The **asymmetrized flux calculation** discretizes $\hat{q}^x$ and $\hat{q}^y$ as

$$\hat{q}^x_{i+\frac{1}{2}j} = \frac{1}{2}\left(q_{i+1j} + q_{ij}\right) - \frac{C_x}{2}\left(q_{i+1j} - q_{ij}\right) - C_y\left(q_{i+1/2j+1/2} - q_{i+1/2j-1/2}\right) \tag{41}$$

$$\hat{q}^y_{ij+\frac{1}{2}} = \frac{1}{2}\left(q_{ij+1} + q_{ij}\right) - \frac{C_y}{2}\left(q_{ij+1} - q_{ij}\right) \tag{42}$$

We follow the computational efficiency comparison of [Zerroukat et al.(2006)] to calculate the number of operations required to calculate the fluxes of both methods, e.g. equations (38)-(39) compared with (41)-(42). The full fluxes require 10 additions and 10 multiplications, giving a total Number of Operations ($NO$) as $NO_{\text{full}} = 20$. The asymmetrized flux calculation requires 8 additions and 7 multiplications, and so $NO_{\text{afc}} = 15$. The ratio of number of operations for the second-order fluxes is $NO_{\text{full}}/NO_{\text{afc}} \approx 1.33$, i.e. the full fluxes are $\approx 33\%$ more expensive than the asymmetrized flux.

Standard truncation error analysis applied to these schemes show that both the full formulation and the asymmetrized flux calculation are formally second-order in space and time.

*A.2. Three-Dimensional Flow*

We can repeat the number of operations calculation for the second-order schemes for the three-dimensional advection equation (27). For this case $\hat{q}^x$ is stored at half $x$ points $(i \pm 1/2, j, k)$, $\hat{q}^y$ is stored at half $y$ points $(i, j \pm 1/2, k)$, and $\hat{q}^z$ is stored at half $z$ points $(i, j, k \pm 1/2)$. We also introduce the Courant number in the $z$ direction, $C_z = w\Delta t/\Delta z$. The tracer is also required at the following points:

$$q_{i+1/2j+1/2k} = \frac{1}{4}\left(q_{ijk} + q_{i+1jk} + q_{ij+1k} + q_{i+1j+1k}\right) \tag{43}$$

$$q_{i+1/2jk+1/2} = \frac{1}{4}\left(q_{ijk} + q_{i+1jk} + q_{ijk+1} + q_{i+1jk+1}\right) \tag{44}$$

$$q_{ij+1/2k+1/2} = \frac{1}{4}\left(q_{ijk} + q_{ij+1k} + q_{ijk+1} + q_{ij+1k+1}\right) \tag{45}$$

The **full flux** terms for the second-order scheme can be discretized using

$$\hat{q}^x_{i+\frac{1}{2}jk} = \frac{1}{2}\left(q_{i+1jk} + q_{ijk}\right) - \frac{C_x}{2}\left(q_{i+1jk} - q_{ijk}\right) - \frac{C_y}{2}\left(q_{i+1/2j+1/2k} - q_{i+1/2j-1/2k}\right) - \frac{C_z}{2}\left(q_{i+1/2jk+1/2} - q_{i+1/2jk-1/2}\right), \tag{46}$$

$$\hat{q}^y_{ij+\frac{1}{2}k} = \frac{1}{2}\left(q_{ij+1k} + q_{ijk}\right) - \frac{C_x}{2}\left(q_{i+1/2j+1/2k} - q_{i-1/2j+1/2k}\right) - \frac{C_y}{2}\left(q_{ij+1k} - q_{ijk}\right) - \frac{C_z}{2}\left(q_{ij+1/2k+1/2} - q_{ij+1/2k-1/2}\right), \tag{47}$$

$$\hat{q}^z_{ijk+\frac{1}{2}} = \frac{1}{2}\left(q_{ijk+1} + q_{ijk}\right) - \frac{C_x}{2}\left(q_{i+1/2jk+1/2} - q_{i-1/2jk+1/2}\right) - \frac{C_y}{2}\left(q_{ij+1/2j+1/2} - q_{ij-1/2k+1/2}\right) - \frac{C_z}{2}\left(q_{ijk+1} - q_{ijk}\right), \tag{48}$$

whereas the **asymmetrized flux calculation** discretizes these as

$$\hat{q}^x_{i+\frac{1}{2}jk} = \frac{1}{2}\left(q_{i+1jk} + q_{ijk}\right) - \frac{C_x}{2}\left(q_{i+1jk} - q_{ijk}\right) - C_y\left(q_{i+1/2j+1/2k} - q_{i+1/2j-1/2k}\right) - C_z\left(q_{i+1/2jk+1/2} - q_{i+1/2jk-1/2}\right), \tag{49}$$

$$\hat{q}^y ij + \frac{1}{2}k = \frac{1}{2}\left(q_{ij+1k} + q_{ijk}\right) - \frac{C_y}{2}\left(q_{ij+1k} - q_{ijk}\right) - C_z\left(q_{ij+1/2k+1/2} - q_{ij+1/2k-1/2}\right), \tag{50}$$

$$\hat{q}^z_{ijk+\frac{1}{2}} = \frac{1}{2}\left(q_{ijk+1} + q_{ijk}\right) - \frac{C_z}{2}\left(q_{ijk+1} - q_{ijk}\right), \tag{51}$$

The computational efficiency comparison shows that the full fluxes, (46)-(48), have a total Number of Operations of $NO_{\text{full}} = 42$ (21 additions and 21 multiplications). The asymmetrized flux calculation, (49)-(51), requires 15 additions and 12 multiplications, and so $NO_{\text{afc}} = 27$. The ratio of number of operations for the second-order fluxes for three-dimensional flow is $NO_{\text{full}}/NO_{\text{afc}} \approx 1.56$, i.e. the full fluxes are $\approx 56\%$ more expensive than the asymmetrized flux.

## B. FOURTH-ORDER DISCRETIZATION

As in A, for demonstrative purposes we will consider the two-dimensional case with constant $u$ and $v$, letting $C_x = u\Delta t/\Delta x$ and $C_y = v\Delta t/\Delta y$.

We use fourth-order interpolations to calculate $q$ at half indices in $x$,

$$q_{i-1/2j} = \frac{1}{12}\left(-q_{i+1j} + 7q_{ij} + 7q_{i-1j} - q_{i-2j}\right), \tag{52}$$

and then repeat this to get $q$ at cell corner points

$$q_{i-1/2j-1/2} = \frac{1}{12}\left(-q_{i-1/2j+1} + 7q_{i-1/2j} + 7q_{i-1/2j-1} - q_{i-1/2j-2}\right). \tag{53}$$

Derivatives of $q$ are calculated at cell centres and at corner points using fourth-order approximations

$$\frac{\partial q_{ij}}{\partial x} = \frac{1}{12}\left(-q_{i+2j} + 8q_{i+1j} - 8q_{i-1j} + q_{i-2j}\right), \tag{54}$$

$$\frac{\partial q_{i-1/2j-1/2}}{\partial x} = \frac{1}{12}\left(-q_{i+2j-1/2} + 8q_{i+1j-1/2} - 8q_{i-1j-1/2} + q_{i-2j-1/2}\right), \tag{55}$$

which can be rotated for $y$ derivates. These can then be applied multiple times to calculate the higher derivatives at these points. Derivatives are also calculated at $F$ flux points

$$\frac{\partial q_{i-1/2j}}{\partial x} = \frac{1}{12}\left(-q_{i+1j} + 15q_{ij} - 15q_{i-1j} + q_{i-2j}\right), \tag{56}$$

$$\frac{\partial q_{i-1/2j}}{\partial y} = \frac{1}{12}\left(-q_{i-1/2j+3/2} + 15q_{i-1/2j+1/2} - 15q_{i-1/2j-1/2} + q_{i-1/2j-3/2}\right), \tag{57}$$

along with the second and third derivatives

$$\frac{\partial^2 q_{i-1/2j}}{\partial x^2} = \frac{1}{2}\left(q_{i+1j} - q_{ij} - q_{i-1j} + q_{i-2j}\right), \tag{58}$$

$$\frac{\partial^3 q_{i-1/2j}}{\partial x^3} = \frac{1}{24}\left(q_{i+1j} - 3q_{ij} + 3q_{i-1j} - q_{i-2j}\right). \tag{59}$$

Again, these can be rotated to give the derivatives at $G$ flux points for $y$ derivatves.

The **full flux** terms for the fourth-order scheme can be discretized using

$$\hat{q}^x_{i+\frac{1}{2}j} = q_{i+1/2j} - \frac{C_x}{2}\frac{\partial q_{i+1/2j}}{\partial x} - \frac{C_y}{2}\frac{\partial q_{i+1/2j}}{\partial y} + \frac{C_x^2}{6}\frac{\partial^2 q_{i+1/2j}}{\partial x^2} + \frac{C_xC_y}{4}\frac{\partial}{\partial x}\left(\frac{\partial q_{ij}}{\partial y}\right) + \frac{C_y^2}{4}\frac{\partial}{\partial y}\left(\frac{\partial q_{i+1/2j+1/2}}{\partial y}\right)$$
$$- \frac{C_x^3}{24}\frac{\partial^3 q_{i+1/2j}}{\partial x^3} - \frac{C_x^2C_y}{12}\frac{\partial^2}{\partial x^2}\left(\frac{\partial q_{ij}}{\partial y}\right) - \frac{C_xC_y^2}{8}\frac{\partial}{\partial x}\left(\frac{\partial^2 q_{ij}}{\partial y^2}\right) - \frac{C_y^3}{12}\frac{\partial^3 q_{i+1/2j}}{\partial y^3} \tag{60}$$

and

$$\hat{q}^y_{ij+\frac{1}{2}j} = q_{ij+1/2} - \frac{C_x}{2}\frac{\partial q_{ij+1/2}}{\partial x} - \frac{C_y}{2}\frac{\partial q_{ij+1/2}}{\partial y} + \frac{C_x^2}{6}\frac{\partial}{\partial x}\left(\frac{\partial q_{i+1/2j+1/2}}{\partial x}\right) + \frac{C_xC_y}{4}\frac{\partial}{\partial y}\left(\frac{\partial q_{ij}}{\partial x}\right) + \frac{C_y^2}{4}\frac{\partial^2 q_{ij+1/2}}{\partial y^2}$$
$$- \frac{C_x^3}{8}\frac{\partial^3 q_{ij+1/2}}{\partial x^3} - \frac{C_x^2C_y}{8}\frac{\partial}{\partial y}\left(\frac{\partial^2 q_{ij}}{\partial x^2}\right) - \frac{C_xC_y^2}{12}\frac{\partial^2}{\partial y^2}\left(\frac{\partial q_{ij}}{\partial x}\right) - \frac{C_y^3}{24}\frac{\partial^3 q_{ij+1/2}}{\partial y^3} \tag{61}$$

The **asymmetrized flux calculation** discretizes $\hat{q}^x$ and $\hat{q}^y$ as

$$\hat{q}^x_{i+\frac{1}{2}j} = q_{i+1/2j} - \frac{C_x}{2}\frac{\partial q_{i+1/2j}}{\partial x} - C_y\frac{\partial q_{i+1/2j}}{\partial y} + \frac{C_x^2}{6}\frac{\partial^2 q_{i+1/2j}}{\partial x^2} + \frac{C_xC_y}{2}\frac{\partial}{\partial x}\left(\frac{\partial q_{ij}}{\partial y}\right) + \frac{C_y^2}{2}\frac{\partial}{\partial y}\left(\frac{\partial q_{i+1/2j+1/2}}{\partial y}\right)$$
$$- \frac{C_x^3}{24}\frac{\partial^3 q_{i+1/2j}}{\partial x^3} - \frac{C_x^2C_y}{6}\frac{\partial^2}{\partial x^2}\left(\frac{\partial q_{ij}}{\partial y}\right) - \frac{C_xC_y^2}{4}\frac{\partial}{\partial x}\left(\frac{\partial^2 q_{ij}}{\partial y^2}\right) - \frac{C_y^3}{6}\frac{\partial^3 q_{i+1/2j}}{\partial y^3} \tag{62}$$

$$\hat{q}^y_{ij+\frac{1}{2}j} = q_{ij+1/2} - \frac{C_y}{2}\frac{\partial q_{ij+1/2}}{\partial y} + \frac{C_y^2}{4}\frac{\partial^2 q_{ij+1/2}}{\partial y^2} - \frac{C_y^3}{24}\frac{\partial^3 q_{ij+1/2}}{\partial y^3} \tag{63}$$

Again, following the computational efficiency comparison of [Zerroukat et al.(2006)] we calculate the number of operations required to calculate the fluxes of both methods. The full fluxes require a total of $NO_{\text{full}} = 230$. The asymmetrized flux calculation requires $NO_{\text{afc}} = 145$. The ratio of number of operations for the second-order fluxes is $NO_{\text{full}}/NO_{\text{afc}} \approx 1.59$, i.e. the full fluxes are $\approx 59\%$ more expensive than the asymmetrized flux. Note that this does not include the operations required for the interpolations. Standard truncation error analysis applied to these schemes show that both the full formulation and the asymmetrized flux calculation are formally fourth-order in space and time.